SANDIA REPORT

SAND2013-9582
Unlimited Release
Printed November 2013

A Feasibility Study for Experimentally Determining Dynamic Force Distribution in a Lap Joint

Randall L. Mayes

Prepared by
Sandia National Laboratories
Albuquerque, New Mexico 87185 and Livermore, California 94550

Sandia National Laboratories is a multi-program laboratory managed and operated by Sandia Corporation, a wholly owned subsidiary of Lockheed Martin Corporation, for the U.S. Department of Energy's National Nuclear Security Administration under contract DE-AC04-94AL85000.

Issued by Sandia National Laboratories, operated for the United States Department of Energy by Sandia Corporation.

NOTICE: This report was prepared as an account of work sponsored by an agency of the United States Government. Neither the United States Government, nor any agency thereof, nor any of their employees, nor any of their contractors, subcontractors, or their employees, make any warranty, express or implied, or assume any legal liability or responsibility for the accuracy, completeness, or usefulness of any information, apparatus, product, or process disclosed, or represent that its use would not infringe privately owned rights. Reference herein to any specific commercial product, process, or service by trade name, trademark, manufacturer, or otherwise, does not necessarily constitute or imply its endorsement, recommendation, or favoring by the United States Government, any agency thereof, or any of their contractors or subcontractors. The views and opinions expressed herein do not necessarily state or reflect those of the United States Government, any agency thereof, or any of their contractors.

SAND2013-9582
Unlimited Release
Printed November 6, 2013

A Feasibility Study for Experimentally Determining Dynamic Force Distribution in a Lap Joint

Randall L. Mayes
Experimental Mechanics/Non-Destructive Evaluation and Model Validation
Sandia National Laboratories P.O. Box 5800
Albuquerque, New Mexico 87185-0557

Abstract

Developing constitutive models of the physics in mechanical joints is currently stymied by inability to measure forces and displacements within the joint. The current state of the art estimates whole joint stiffness and energy loss per cycle from external measured force input and one or two acceleration responses. To validate constitutive models beyond this state requires a measurement of the distributed forces and displacements at the joint interface. Unfortunately, introducing measurement devices at the interface completely disrupts the desired physics. A feasibility study is presented for a non-intrusive method of solving for the interface dynamic forces from an inverse problem using full field measured responses. The responses come from the viewable surface of a beam. The noise levels associated with digital image correlation and continuous scanning laser Doppler velocimetry are evaluated from typical beam experiments. Two inverse problems are simulated. One utilizes the extended Sum of Weighted Accelerations Technique (SWAT). The second is a new approach dubbed the method of truncated orthogonal forces. These methods are much more robust if the contact patch geometry is well identified. Various approaches to identifying the contact patch are investigated, including ion marker tracking, Prussian blue and ultrasonic measurements. A typical experiment is conceived for a beam which has a lap joint at one end with a single bolt connecting it to another identical beam. In a virtual test using the beam finite element analysis, it appears that the SWAT inverse method requires evaluation of too many coefficients to adequately identify the force distribution to be viable. However, the method of truncated orthogonal forces appears viable with current digital image correlation (and probably other) imaging techniques.

ACKNOWLEDGMENTS

The author gratefully acknowledges the people from Sandia National Laboratories, Albuquerque, who performed the experiments, analyses and literature review to support this study. Sharlotte Bolyard Kramer, Mathew Ingraham, John Laing and Phillip Reu provided support, experimental setup, data analysis and literature review for the digital image correlation and related studies on beam deflection experiments. Khalid Hattar and Enrico Quintana provided ion implants using particle accelerators and X-ray and computed tomography imaging of the aluminum plates. Ciji Nelson provided the ultrasonic testing to determine contact area between bolted aluminum plates. Jack Heister provided the design of the aluminum plates and the contact studies for bolted aluminum plates using Prussian blue. David Manko provided static beam analysis. From the University of Wisconsin in Madison, Shifei Yang and Matthew Allen provided the dynamic beam experiments and data analysis using continuous scanning laser Doppler velocimetry. This work was funded under LDRD Project Number165659 and Title "Development of Non-Intrusive Methods to Measure Static and Dynamic Forces and Motions in Mechanical Joints".

CONTENTS

FIGURES

1. INTRODUCTION

Modeling of joints is the weakest link in structural analysis. This LDRD studied the feasibility of providing non-intrusive measured interface force and displacement data to develop first principle constitutive models that currently do not exist. The need is highlighted by a quote from the 2nd Workshop on Joints Modeling, Dartington Hall, UK, where it was stated that "the greatest experimental challenge to joint interface research is obtaining a measurement of the distribution of local interface forces in the joint." Figure 1 shows a loaded lap joint. During the loading process, there is a contact patch in which part of the area is slipping and part is not. Furthermore, the contact area and forces change with load. No sensor is currently available to measure the contact patch force and motion without changing the joint dynamics. These data are required for understanding and modeling structural joints.

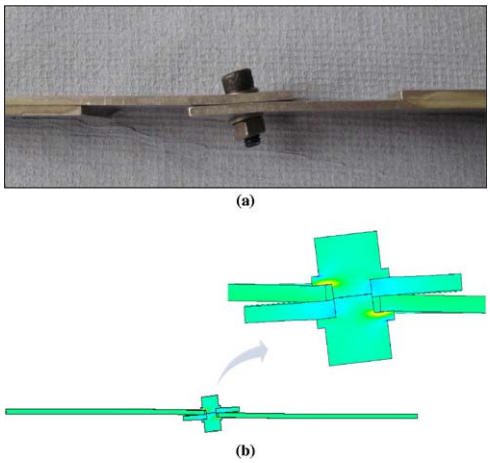

Figure 1 – Lap joint hardware and model with large static tensile load

This LDRD proposed assessing feasibility of non-intrusive measurements of the contact patch motion and dynamic forces without compromising the joint physics. The current state of the art only measures the force applied to the joint hardware and a single displacement across the joint to determine stiffness and energy dissipation per cycle of vibration[1,2], but does not obtain any information on the force or displacement *field* at the interface. This is key to understanding the physics of joint dynamics so that appropriate constitutive models can be discovered. The proposed development would advance validation of joint constitutive model theory, benefitting weapons programs that could then apply such models to their hardware. This report first discusses sensor technologies to gather data non-intrusively and then the algorithms which could be utilized to extract the forces in the contact patch. Section 2 provides the studies that were performed to sense the contact area and its motion. Section 3 deals with gathering digital image correlation (DIC) data from typical beam experiments, and section 4 does the same using continuous scanning laser Doppler velocimetry (CSLDV) to gather the data. Section 5 proposes an experimental setup for which the joint forces would be investigated. Section 6 shows the results of the virtual experiment using the extended SWAT technique to reconstruct the force distribution, and section 7 shows a much more successful technique for reconstructing the force distribution. The final conclusions are presented in section 8.

2. CONTACT AREA STUDIES FOR A BOLTED LAP JOINT

The determination of the contact area would provide one metric for assessing a constitutive model in a finite element code. In addition, force algorithms only need be applied in the contact area, so knowing the contact area would be extremely beneficial. Multiple methods were investigated to determine the static contact area of a bolted joint without violating the joint. One attractive idea was to implant ion markers beneath the interface surface of the material in a lap joint. Here we chose aluminum as the material for two plates 2" x 1" x 0.1" which could be utilized to form a bolted lap joint with a nominal 1 square inch overlap. Sample plates were masked and implanted using particle accelerators with either helium or gold ions with various energy levels and dose rates. Then the plates were viewed under x-ray and mapped with computed tomography (CT). However, even with the highest dose rates utilized for long times, the imaging could only identify an indistinct zone of the implanted gold ions and not specific distinct marks, as necessary for tracking images. With the small displacements that would be imposed statically in a joint, this appeared unfeasible as a contact tracking algorithm. A picture of the highest dose image (white shows the area of ion implants) is shown in the CT scan of Figure 2.

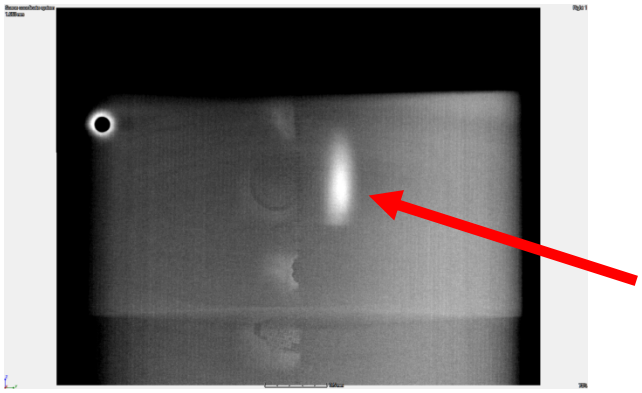

Figure 2 – First layer CT scan of aluminum plate

Several plates were painted with Prussian blue on one surface and then bolted with different torque levels (finger tight, 5, 10, 15, 20 in-lb) to see how the ink transferred to the other interface. This provided insight as to the contact area. One of the many samples is shown in Figure 3. The plate on the right to which the ink transferred shows there are contact areas over the entire one square inch overlap, with more toward the center where the bolt was located. Although there were differences from sample to sample, this shows the general trend, with more ink transferred for higher torques.

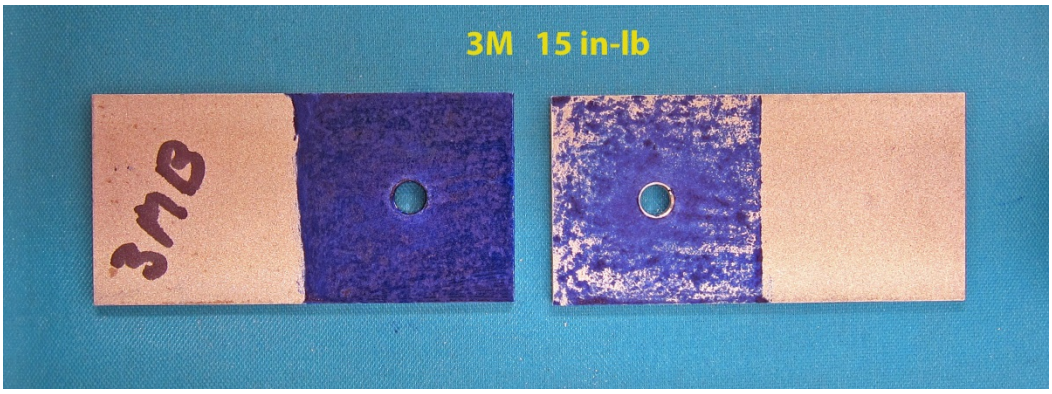

Figure 3 – Contact area for one moderate torque level from Prussian blue ink transfer

Ultrasonic scans were also conducted for ¼ of the contact area. Here the two plates were bolted together and submerged. Ultrasonic signals were imparted and the reflections showed the degree of contact with the plate beneath it. Figure 4 shows the scan for one setup over one quarter of the overlap area. The hole for the bolt is shown in black. Red would indicate full contact and black would indicate little contact. The scan showed some contact over most of the overlap area.

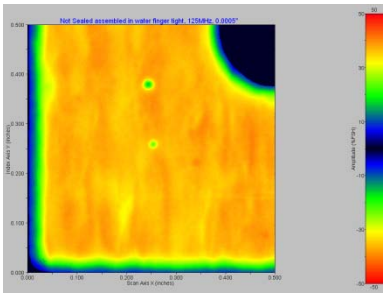

Figure 4 – Ultrasonic scan showing some contact over most of overlap area

The results of both the ultrasonic and Prussian blue testing indicate we could get some quantification of the initial static contact area in a lap joint with these methods.

3. DIGITAL IMAGE CORRELATION ON STATIC BEAM TESTS

Two similar beam configurations were conceived to provide static test environments on which digital image correlation (DIC) could be applied to measure full field displacement. Figure 5 shows the elevation view schematic of the static test concept. An aluminum beam one inch wide, 0.125 inches thick and ten inches long was clamped at one end, simply supported at center span with a static force was applied at the other end. Figure 6 shows the plan view of the beam hardware with the speckle pattern applied to the beam for the DIC study. A second similar test setup had a two inch long, one inch wide, 0.0625 inch thick plate inserted between the simple support and the beam to spread the load acting on the beam from the simple support.

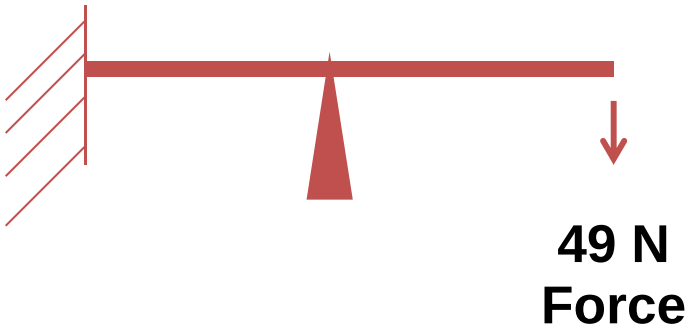

Figure 5 – Static beam test schematic

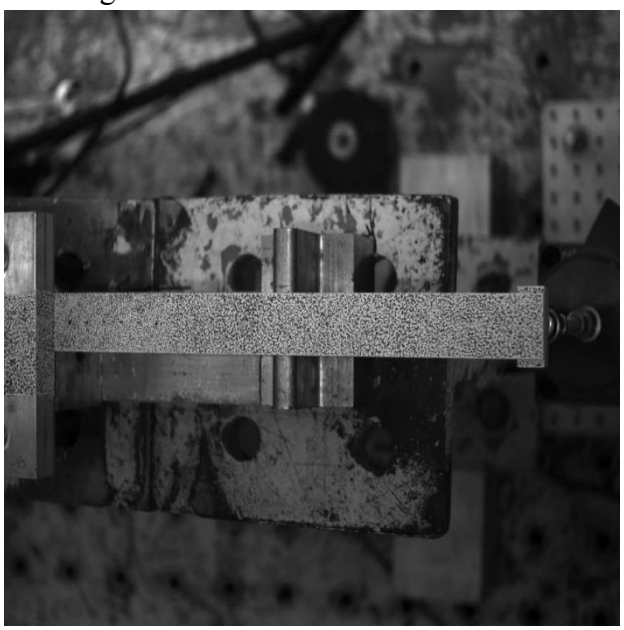

Figure 6 – Plan view of beam static test setup with speckle pattern on beam for DIC

DIC was performed for the static test configuration both with and without the spreader plate. The beam was divided into 300 subsets along the length and 23 subsets across the width. Then all the subsets across the width were averaged to reduce the noise, with the assumption that the

response across the width should be the same. The DIC deflection for both tests is shown in Figure 7. Experimentalists determined that the noise on the deflection measurements of Figure 7 was about 0.008 mm standard deviation on a subset. By averaging across the beam, this equates to about 0.025% of the signal at the beam tip.

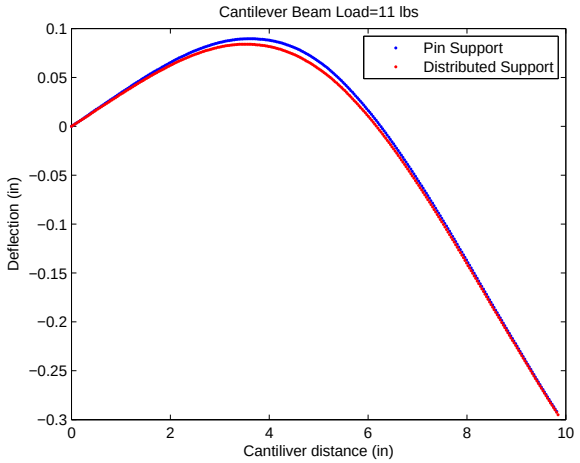

Figure 7 – DIC deflection for two static beam test configurations

Another possible inverse problem is to calculate moments, shears and load per unit length using one of the beam theories and the DIC displacements. If Bernoulli-Euler theory was used, the second, third and fourth derivative of displacement provides moment, shear and load per unit length in the vertical direction. Figure 8 shows the results for 2nd derivative with the simplest finite difference approach, which would clearly be unusable for the inverse problem. If more sophisticated derivative calculations are utilized, which basically provide more averaging, one can theoretically get some reasonable information about the forces in the vertical direction. The more averaging that is required, the less distinct will be the spatial distribution. For example, if one uses a ninth order polynomial to represent the displacement, the error for each of the 300 subsets is averaged out over calculation of ten coefficients, which could provide a fairly accurate estimate of the fourth derivative, but averaged over about a 10 percent length of the beam. This provides a fairly blurry estimate of the force per unit length that might be applied with the two inch long spreader plate. It appears that we are on the edge of feasibility for the vertical direction force calculation with inverse analysis based on one of the beam theories.

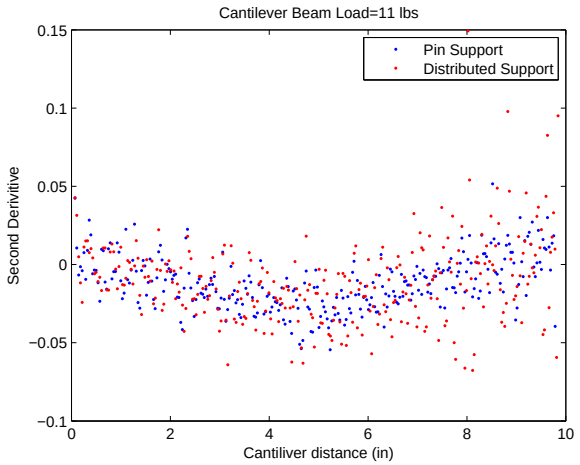

Figure 8 – Most simple finite difference calculation for second derivative of beam vertical displacement

4. CONTINUOUS SCAN LASER DOPPLER VELOCIMETRY (CSLDV) FOR DYNAMIC BEAM EXPERIMENTS

The beam previously described in the DIC static test section was set up in a very similar configuration at University of Wisconsin – Madison laboratories. A similar schematic is shown in Figure 9. However, the beam extension from the clamped support is 10.5 inches instead of 10 inches as before. Also, the beam is excited dynamically with a sinusoidal force of 7 N amplitude at 20 cycles per second. Both the simple support and the two inch long spreader plate configurations were tested. Figure 10 and Figure 11 show the elevation and plan view setup. Figure 11 depicts the view the laser head had as it scanned back and forth down the length of the beam.

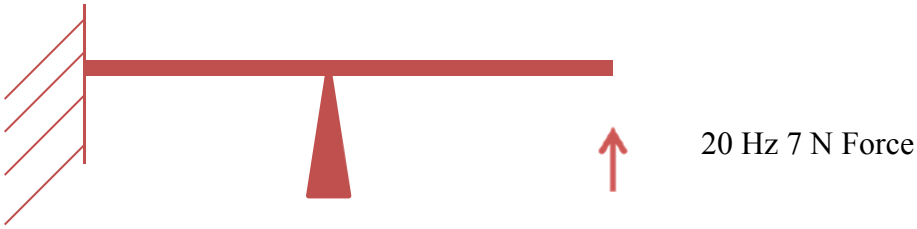

Figure 9 – Schematic of CSLDV test setup

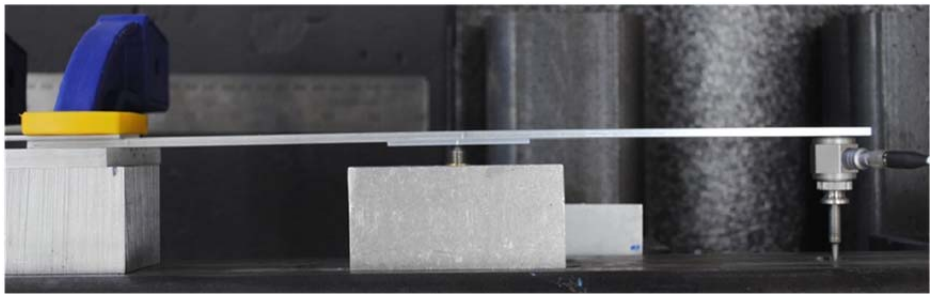

Figure 10 – Elevation view of CSLDV test setup with spreader plate

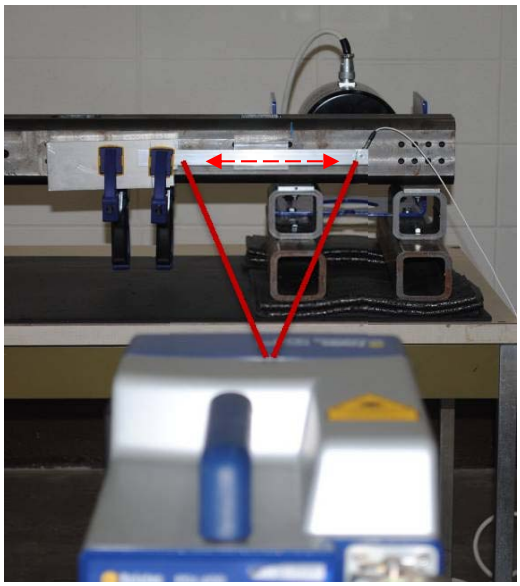

Figure 11 – Top view of CSLDV setup with laser scan location identified

The sinusoidal force was applied to the tip of the beam and a time history of the velocity was obtained over 102 seconds while the laser scanned the length of the beam right and left three times per second. The sample rate is such that velocities at 1700 locations along the beam are sampled. The magnitude of the autospectrum of this time history is shown in Figure 12. The largest peak is seen at 20 Hz which is the forcing frequency. A pair of side lobes is observed at multiples of the 3 Hz scan frequency on both the right and left sides of the main peak. These side lobe amplitudes are converted to coefficients of a polynomial in beam length x that describe the motion of the beam. The amplitude plot related to this polynomial is shown in Figure 13 for both the simple support and the spreader configurations.

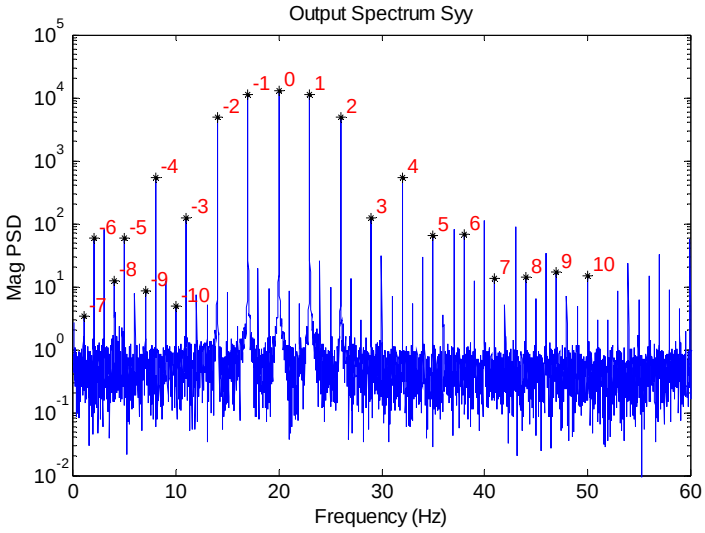

Figure 12 – Autospectrum of CSLDV velocity time history

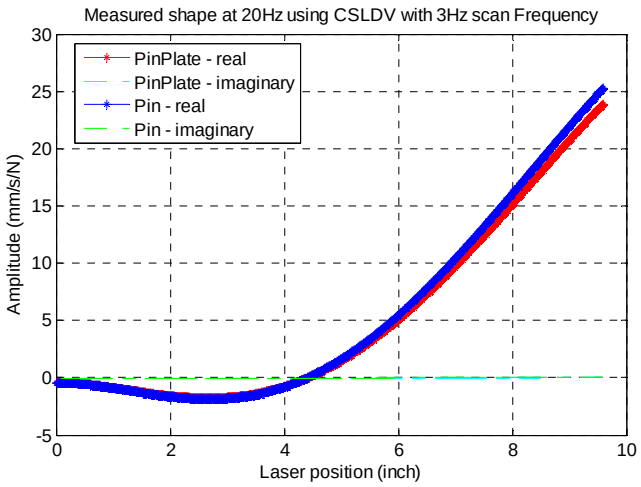

Figure 13 – CSLDV displacement plot for test beams

There is speckle noise in the velocity signal. Averaging the shape sampled over the 102 seconds produces a standard deviation that is about 0.026% of the largest velocity at the beam tip. The speckle noise occurs mostly at integer multiples of the scan frequency, in this case 0,3,6,9… Hz. By appropriate setting of the sinusoidal input frequency and the scan frequency, the side lobe amplitudes are at different frequencies than the speckle noise spikes. This reduces the effect of the speckle noise on the shape calculation. Wisconsin researchers analyzing this data believe that one can use about seven pairs of the side lobes before one begins to get close to the noise floor. So theoretically, estimates of a smooth polynomial fit to the shape can easily predict a second, third and fourth derivative for use in force calculations using the inverse beam theory. The second derivative (which is proportional to moment) plot is shown in Figure 14.

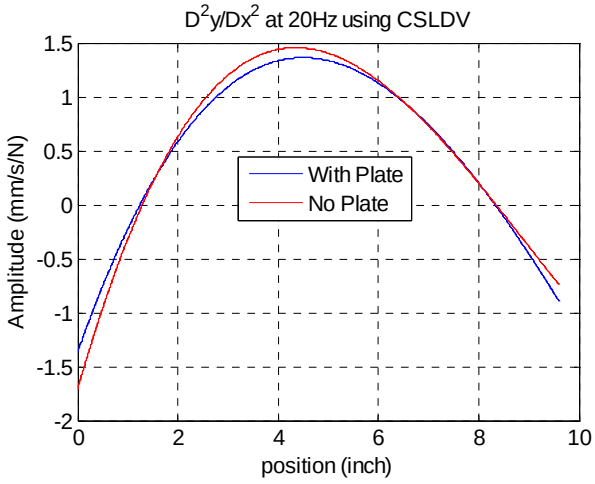

Figure 14 – Second derivative of CSLDV displacement

The disadvantage of utilizing the polynomial solution is that it does not capture local instantaneous discontinuities in moment, shear or load per unit inch since the polynomial is by definition a smooth curve with no discontinuities. Therefore, local instantaneous changes in force distribution, such as one would have at each end of the spreader plate will be blurred without a very large number of polynomial coefficients. However, some information about the load distribution is contained for the vertical motion in these velocity plots. This method is also producing dynamic information, not just static information. It may be feasible with this method to provide an inverse calculation to estimate vertical forces from beam theory.

5. VIRTUAL LAP JOINT FORCE RECONSTRUCTION EXPERIMENT

A virtual experiment was envisioned which could be used to gather full field data for use in solving the inverse problem of the force distribution in the contact area of a lap joint. A finite element model (FEM) of the beam was developed to perform the virtual experiment. The two dimensional problem is shown in Figure 15. The structure would be two beams with end masses supported by soft bungee cords in a near free configuration. A single bolt would attach the two beams together. A sinusoidal forcing function, F, would be applied near the center of gravity of one mass/beam. A full field sensor could capture response on the top surface and sides of the red beam/mass. The goal would be to reconstruct the forces being applied by the blue beam through the contact area to the red beam. This system could be designed such that the first elastic mode of the system could be excited by providing the appropriate sinusoidal forcing frequency for F. This would allow relatively large deflections to be realized for small force inputs by exciting near the resonant frequency. The first mode of vibration would have the nice feature of applying large shear forces to the red beam in the contact patch which would enhance micro-slip type behavior, the type of behavior for which we need to develop/validate constitutive models.

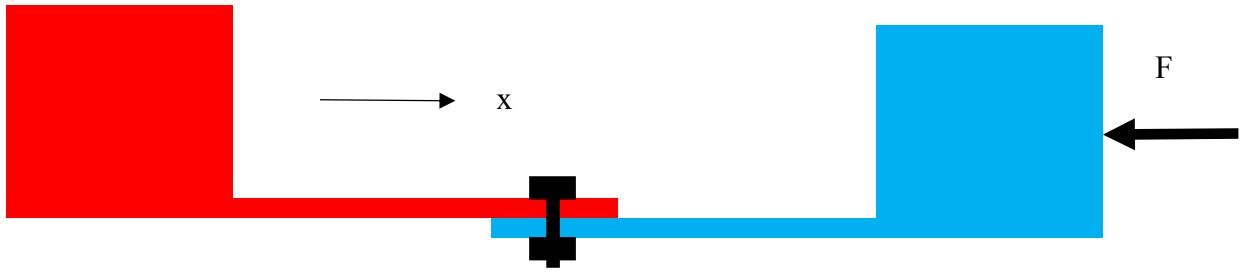

Figure 15 – Proposed lap joint system for the inverse force reconstruction

The two dimensional problem was simulated with a finite element beam model in MATLAB. Several geometries were attempted, but the one that met with some success was based on the beams and masses made from aluminum, two inch long beams with a one inch overlap at the bolted joint, large masses of about 30 pounds weight to bring the system first elastic mode down to about 20 Hz. The sinusoidal force applied would be on the order of 20 to 50 pounds peak, and it would be applied just far enough off the resonant frequency that damping could be neglected for the steady state response. Imaging of the entire top surface of the red beam would be envisioned with the results averaged down to 41 nodes that correspond to the 41 nodes of a FEM of the beam.

6. FEASIBILITY OF DETERMING INTERFACE CONTACT FORCES WITH THE EXTENDED SUM OF WEIGHTED ACCELERATIONS TECHNIQUE

Using the same FEM from the previous section, a truth set of smoothly varying horizontal, vertical and moment forces were applied to the contact area of the red beam. To attempt to predict these truth forces, the extended sum of weighted accelerations technique (SWAT) was applied using noise free full field horizontal and vertical displacements obtained at each node of the red beam FEM. The SWAT technique[3,4] was developed by multiple researchers at Sandia labs in the 80's and 90's and is a very robust method for obtaining the sum of all forces on a structure from an array of point acceleration responses. It does not determine the distribution of forces. However, the theory of SWAT was extended by Genaro and Rade[5] to extend the capability to approximate the force distributions. The theory is briefly developed below.

$$M\bar{\ddot{u}} + C\bar{\dot{u}} + K\bar{u} = \bar{f} \tag{1}$$

$$M\Phi\bar{\ddot{q}} + C\Phi\bar{\dot{q}} + K\Phi\bar{q} = \bar{f} \tag{2}$$

$$\Phi^T M\Phi\bar{\ddot{q}} + \Phi^T C\Phi\bar{\dot{q}} + \Phi^T K\Phi\bar{q} = \Phi^T\bar{f} \tag{3}$$

$$\begin{bmatrix} I & 0 \\ 0 & I \end{bmatrix}\bar{\ddot{q}} + \begin{bmatrix} I & 0 \\ 0 & 2\zeta_n\omega_n \end{bmatrix}\bar{\dot{q}} + \begin{bmatrix} 0 & 0 \\ 0 & \omega_n^2 \end{bmatrix}\bar{q} = \Phi^T\bar{f}(\omega) \tag{4}$$

$$\Phi^{T+}\begin{bmatrix} -I\omega^2 & 0 \\ 0 & \omega_n^2 + j2\zeta_n\omega\omega_n - I\omega^2 \end{bmatrix}\Phi^{+}\bar{u}(\omega) = \bar{f}(\omega) \tag{5}$$

M,C and *K* are the mass, stiffness and damping matrices. The force vector is represented by *f* and the displacement vector by *u*. Generalized displacements are represented by *q*. The mode shape matrix is given by Φ, and ζ_n represents the modal damping ratio, while ω_n represents the system natural frequency, and ω represents any frequency in which there is excitation. Standard SWAT uses the upper row of eqn (5). The extended SWAT utilizes the additional partition of the second row of eqn(5).

The "truth" forces of Figure 16 were applied to the contact area on the red beam FEM. Vertical forces are in the top plot, horizontal forces in the second plot and moments in the third plot.

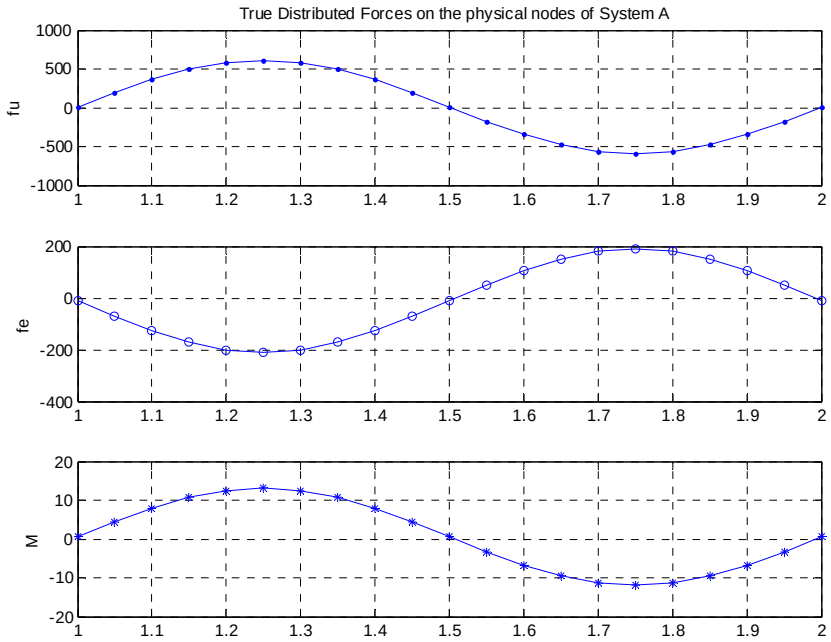

Figure 16 – True forces imposed on contact area of red beam FEM

Genaro and Rade's extended SWAT calculation was used to estimate the force in the contact area. I was expected that only the lower frequency modes would contribute strongly to the solution so that a truncated set of the modes could achieve an accurate force reconstruction. The first attempt utilized 15 modes of the red beam and its result is shown in Figure 17. Here the result has nearly converged to the true horizontal force distribution (middle plot), but the vertical forces and moments are off by a factor of 10 and have the wrong distribution. In Figure 18, the result is displayed retaining 75 modes. Again the horizontal force is accurate, but the vertical forces and moments are off by several orders of magnitude and have wildly oscillating distributions. Finally in Figure 19, the result using almost every mode of the FEM converges to the "right" answer. However, real experimental data will have noise on the displacement vector. The multipliers on the displacement vector in the lower row of eqn (5) are the square of the circular natural frequency. These multipliers on the noise become astronomical after only a half dozen modes. This method is practically infeasible for this example, because the vertical forces and moments do not monotonically converge on the answer, but actually diverge until nearly all terms are gathered.

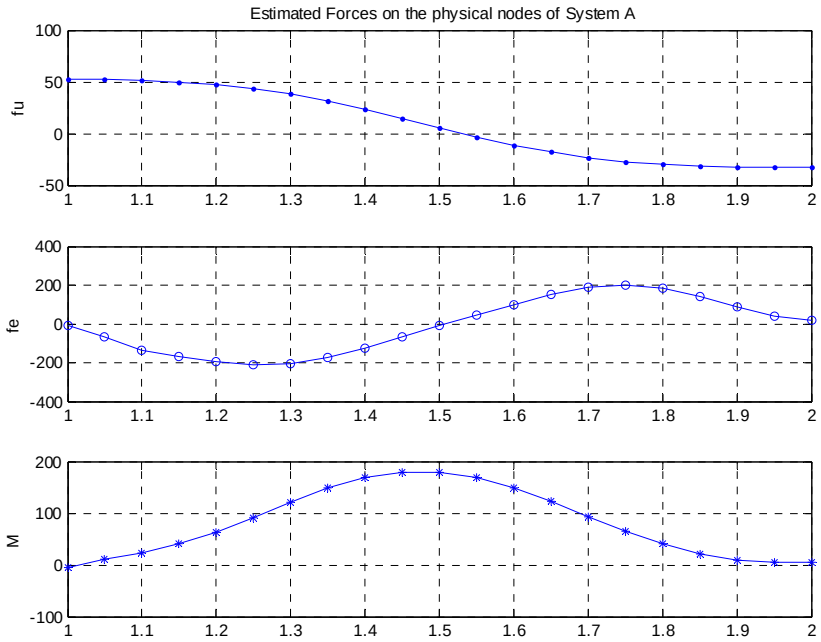

Figure 17 – 15 mode force approximation

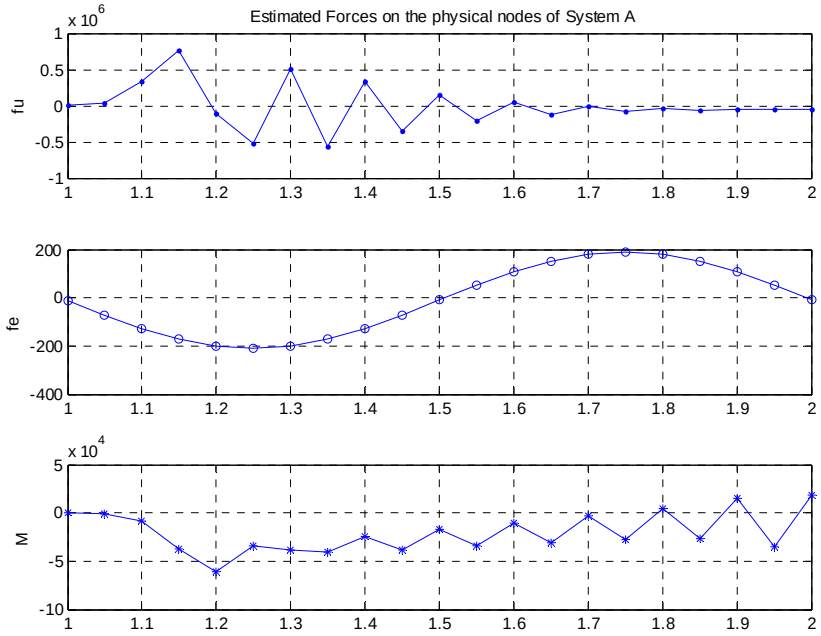

Figure 18 – 75 mode force approximation

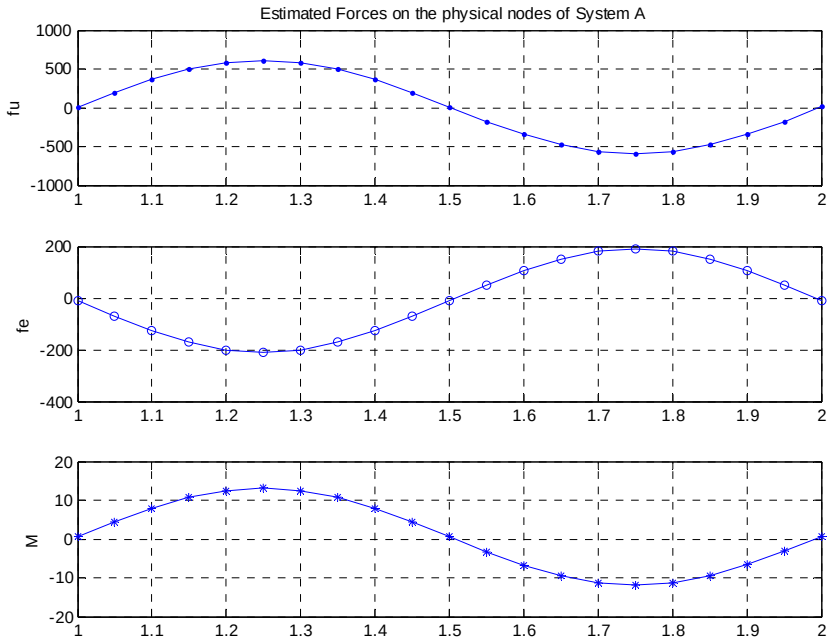

Figure 19 – 120 mode force approximation

Perhaps this is the reason that there is not widespread use of Genaro and Rade's method. For this problem, the method of standard SWAT works well to determine the *sum* of the forces, but as soon as any additional rows of eqn (5) are added to determine the distributions, the vertical forces and moments begin to diverge. In a practical implementation, even 15 modes would be a large number to retain, and could be amplifying noise on the displacement vector data. This exercise indicated that extended SWAT was not viable for this process.

7. METHOD OF TRUNCATED ORTHOGONAL FORCES

Since the extended SWAT technique did not work, a different algorithm was conceived and dubbed the method of truncated orthogonal forces, which was implemented with promise on the FEM. It has some similarities to the extended SWAT technique, but turned out to be much more stable. In this method we first discretize the forces in the contact area at the nodes of the finite element model. It is known that the forces in the vertical and horizontal directions can be represented by a weighted sum of orthogonal vectors. In this case a Fourier series was chosen as the set of orthogonal vectors to represent the vertical and the horizontal force distribution. This expresses the force in one direction as a sum of a constant and sines and cosines as a function of the distance along the beam axis. The orthogonal vectors can be summed together with appropriate coefficients to obtain a force reconstruction. When the number of orthogonal vectors is equal to the number of discretized forces, the solution is exact. However, it is envisioned that in practice a truncated set of orthogonal vectors will be sufficient to describe the force distribution. In addition, noise on the measured data will make higher order terms of the series very uncertain. In this case, each orthogonal force vector was applied to the model, and the corresponding displacement shape was obtained. These corresponding shapes were incorporated with simulated test data of the vertical and in plane responses including noise similar to the noise we obtained using DIC in the lab. The data were averaged over time and spatially to obtain the vertical and horizontal displacements at the 41 axial locations of the FEM of the red beam, Figure 14. This averaged response was then utilized with the equations of motion and the characteristic shapes to estimate the force as a sum of the weighted truncated orthogonal vectors. Reconstructed forces (red) are compared with four truth force distributions (blue) in the following figures. First, a force was assumed in both directions that was a constant plus a sine wave in the x direction. These are two of the truncated orthogonal shape vectors, so they should be reconstructed with least difficulty. Figure 20 shows that with the averaging previously described, the reconstructed force is very accurate. f_u is the vertical force, f_e is the horizontal (extensional) force and M is the moment.

The next assumed force distribution is a shifted triangle wave with one period for the horizontal force direction. This should not be able to be reproduced exactly with the truncated number of sines and cosines, and the result is shown in Figure 21.

Now consider a horizontal force assumption with the triangle wave distorted on one end as shown in Figure 22.

Finally consider an assumed distorted triangle wave in the vertical force assumption in Figure 23.

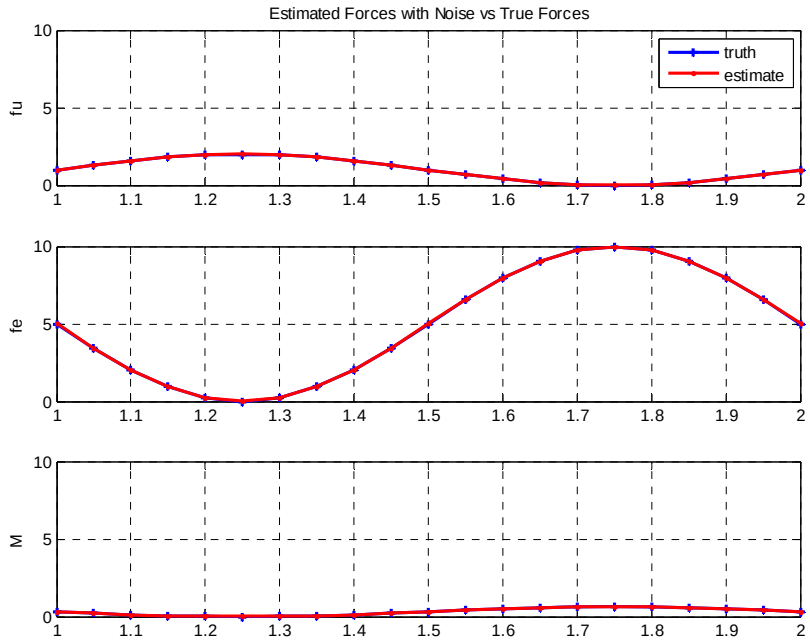

Figure 20 – Assumed force is a sine wave plus constant (blue) and reconstruction (red) utilizing three Fourier series terms and 100 virtual DIC images with noise

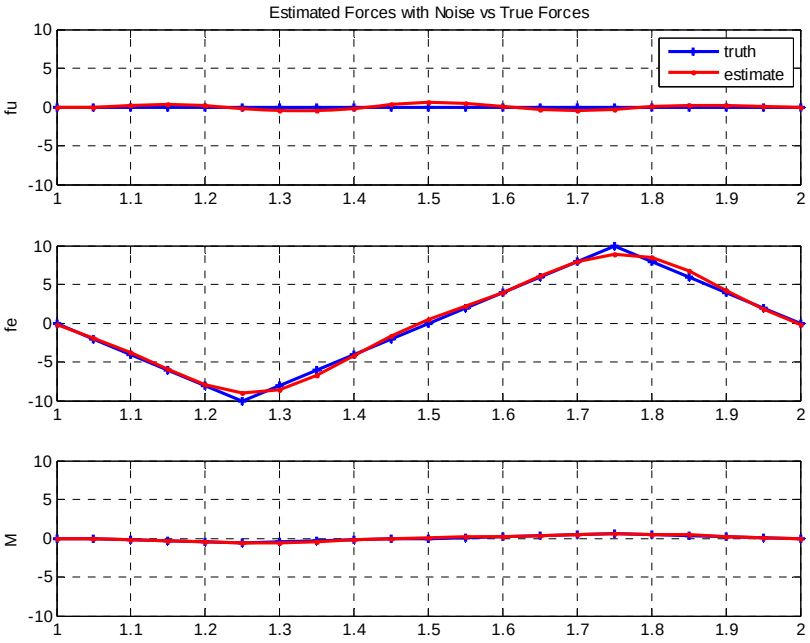

Figure 21 – Assumed force is a shifted triangle wave (blue) with reconstruction (red) using 7 Fourier series terms and 10,000 virtual DIC images with noise

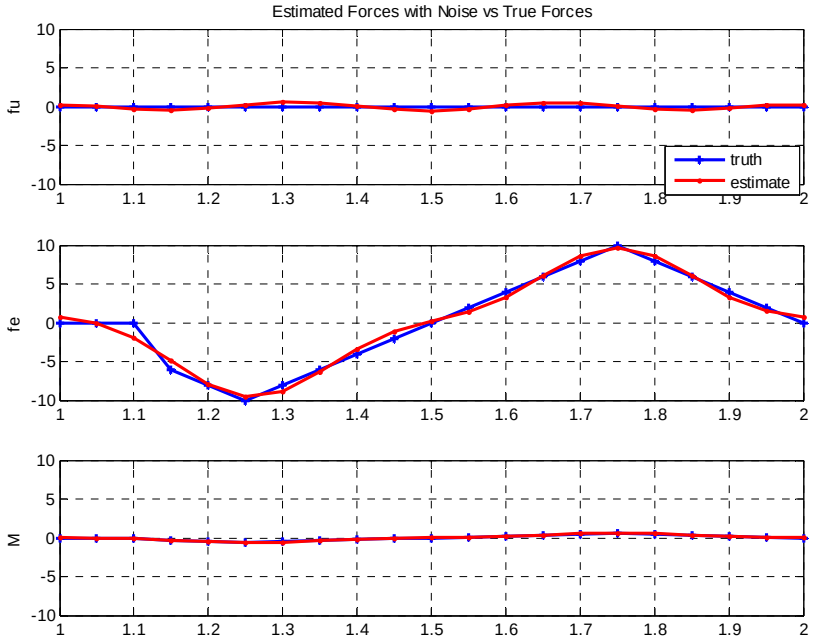

Figure 22 – Assumed distorted triangle wave in axial force (blue) with reconstruction (red) with 7 Fourier series terms and 10,000 virtual DIC images with noise

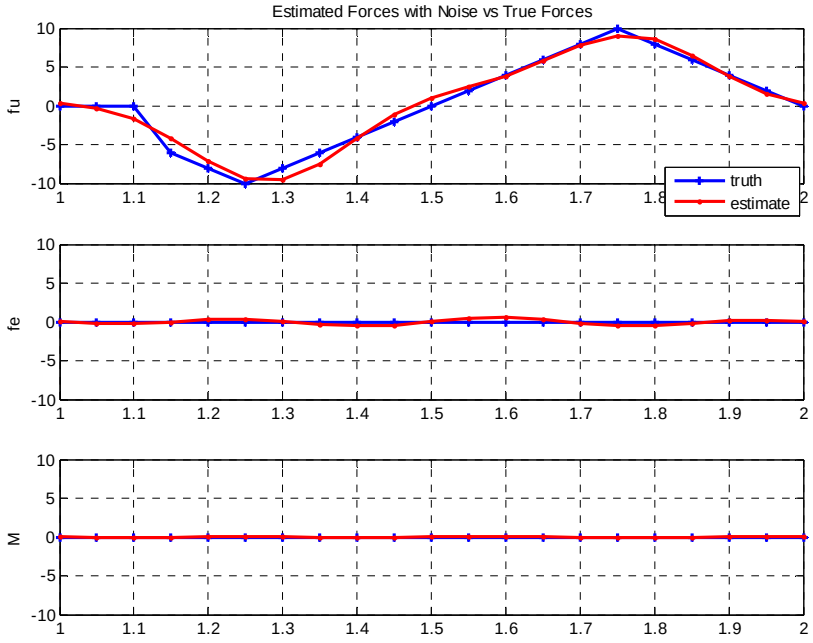

Figure 23 – Assumed distorted triangle wave in vertical force (blue) with reconstruction (red) with 7 Fourier series terms and 10,000 virtual DIC images with noise

The theory to obtain force reconstruction with truncated orthogonal forces begins with the equations of motion, repeated here for convenience.

$$M\ddot{\bar{u}} + C\dot{\bar{u}} + K\bar{u} = \bar{f} \tag{6}$$

Exciting the system off resonance with a sinusoidal force for a structure made of one piece aluminum with low damping, the damping term can be ignored. Transforming into the frequency domain for convenience yields

$$[-\omega^2 M + K]\bar{u} = \bar{f} \quad . \tag{7}$$

Select a truncated set of orthogonal force vectors which shall be retained as a matrix F. (In our case we selected terms of a Fourier series in x). Apply each column of F to obtain a response vector u. Each response vector shall be placed in a matrix Γ. Measure the available DoF, which is a subset of all DoF of the FEM. For example, in this case all rotations are unmeasured. Approximate the full *u* vector as

$$\bar{u} = \Gamma\Gamma_m^+ \bar{u}_m \tag{8}$$

where the *m* subscript indicates the measured DoF. Substituting eqn (8) into eqn(7) yields

$$[-\omega^2 M + K]\Gamma\Gamma_m^+ \bar{u}_m = \bar{f} \quad . \tag{9}$$

The resulting *f* vector will be constrained in the vector space of matrix F. If more vectors are added to F, the solution can be more spatially refined, but typically becomes more unstable due to experimental noise errors. The solution will converge if the noise is reduced enough (for example, by averaging).

For the beam analysis, the approximate number of images that were required to average out random noise and get a converged force reconstruction was related to the number of terms retained in the Fourier series as given below.

No. terms for both vertical and horizontal truncated vectors	No. images required
3	100
5	1000
7	10,000

This tradeoff will impact the test setup and data processing resource requirements. DIC analysts say that 10,000 images can be processed in an overnight computer run, which is quite feasible.

8. CONCLUSIONS

In conclusion, the method of truncated orthogonal forces conditions the inverse problem in a manner that proved viable in a virtual test (based on a FEM) for a logistically practical experimental setup with noise levels consistent with standard DIC approaches. Thus the non-intrusive approach now appears feasible with DIC and possibly other imaging technologies in which at least two dimensional (out of plane and in-plane in direction of applied force) full field displacement data may be acquired. It appears that the extended SWAT methodology is not feasible using full field data, as for the best virtual experiment that was conceived the method failed for a reasonable number of retained modes, even with perfect response data from the FEM.

For solving an inverse problem directly from beam theory, the DIC and CSLDV appear to be able to provide fairly low noise out of plane deflection data for full field type measurements. These might be applicable for determining vertical forces for an inverse problem using beam theory, although resources did not allow us to determine this viability for an example problem. There are some potential improvements that might reduce the noise even further. For example, after this study, it appears that it might be better to focus in on the contact patch portion of the beam instead of the entire beam. DIC has better resolution in the horizontal direction than the vertical, which appeared to be enough for the virtual test configuration. CSLDV had slightly better vertical response results than the DIC, and the data analysis is designed for dynamic analysis. However, CSLDV requires a more exotic two or three laser setup to obtain three dimensional response, which is already standard in DIC 2 camera systems. Both technologies deserve further investigation if a future LDRD is allowed to proceed.

Using either Prussian blue ink or ultrasonic scanning techniques provided an estimate of the contact area for the statically bolted lap joint. Dynamic measurements of the contact area displacements are still an open question.

9. REFERENCES

[1] Segalman, D, Gregory, D, Starr, M, Resor, B, Jew, M, Lauffer, J, Ames, N (2009) Handbook on Dynamics of Jointed Structures. Sandia Report SAND2009-4164 :1-530
[2] Bograd, S, Reuss, P, Schmidt, A, Gaul, L, Mayer, M (2011) Modeling the dynamics of mechanical joints. Mech Sys and Signal Proc 25:2827-2848
[3] Bateman, V, Mayes, R, Carne, T (1997) Comparison of Force Reconstructon Methods for a Lumped Mass Beam. Shock and Vibration Vol 4 No 4:231-239
[4] Mayes, R (1994) Measurement of Lateral Launch Loads on Re-entry Vehicles Using SWAT. 12th IMAC Proceedings 1063-1068
[5] Genaro, G, Rade, D (1998) Input Force Identification in the Time Domain. 16th IMAC Proceedings 124-129.

DISTRIBUTION

1	MS0346	Michael A. Guthrie	1523
1	MS0346	Mikhail Mesh	1523
1	MS0346	Michael J. Starr	1526
1	MS0359	Donna L. Chavez	7911
1	MS0557	C. Dennis Croessmann	1520
1	MS0557	David Epp	1522
1	MS0557	Laura D. Jacobs-O'Malley	1521
1	MS0557	Sharlotte Kramer	1522
1	MS0557	Randall L. Mayes	1522
1	MS0557	Tyler Schoenherr	1522
1	MS0557	Todd Simmermacher	1523
1	MS1070	Matthew R. Brake	1526
1	MS1139	Phillip L. Reu	1535
1	MS9042	Daniel J. Segalman	8259

1	MS0899	Technical Library	9536 (electronic copy)


Sandia National Laboratories